

# Characterization and Tests of Different Mach-Zehnder Silicon Photonic Modulator Configurations

Davide Badoni<sup>1,a\*</sup>, Vincenzo Bonaiuto<sup>2,b</sup>, Mauro Casalboni<sup>2,c</sup>, Fabio De Matteis<sup>2,d</sup>,  
Giovanni Di Giuseppe<sup>3,e</sup>, Luca Frontini<sup>4,f</sup>, Roberto Gunnella<sup>3,g</sup>,  
Valentino Liberali<sup>5,h</sup>, Andreas Mai<sup>6,i</sup>, Giovanni Paoluzzi<sup>1,j</sup>, Paolo Proposito<sup>2,k</sup>,  
Andrea Salamon<sup>1,l</sup>, Gaetano Salina<sup>1,m</sup>, Fausto Sargeni<sup>2,n</sup>, Sigurd Schrader<sup>7,o</sup>,  
Alberto Stabile<sup>5,p</sup>, Patrick Steglich<sup>6,7,q</sup>

<sup>1</sup>INFN Structure of Rome Tor Vergata, Rome, Italy

<sup>2</sup>University of Rome Tor Vergata, Rome, Italy

<sup>3</sup>University of Camerino, Macerata, Italy

<sup>4</sup>INFN Structure of Milano, Milan, Italy

<sup>5</sup>University of Milano, Milan, Italy

<sup>6</sup>IHP – Innovations for High Performance Microelectronics, Frankfurt (Oder), Germany

<sup>7</sup>Technical University of Applied Sciences Wildau, Wildau, Germany

<sup>a</sup>davide.badoni@roma2.infn.it, <sup>b</sup>vincenzo.bonaiuto@uniroma2.it,

<sup>c</sup>mauro.casalboni@roma2.infn.it, <sup>d</sup>fabio.dematteis@roma2.infn.it,

<sup>e</sup>gianni.digiuseppe@unicam.it, <sup>f</sup>luca.frontini@mi.infn.it, <sup>g</sup>roberto.gunnella@unicam.it,

<sup>h</sup>valentino.liberali@mi.infn.it, <sup>i</sup>andreas.mai@ihp-microelectronics.com,

<sup>j</sup>giovanni.paoluzzi@roma2.infn.it, <sup>k</sup>paolo.proposito@roma2.infn.it,

<sup>l</sup>andrea.salamon@roma2.infn.it, <sup>m</sup>gaetano.salina@roma2.infn.it,

<sup>n</sup>fausto.sargeni@uniroma2.it, <sup>o</sup>schrader@th-wildau.de, <sup>p</sup>alberto.stabile@mi.infn.it,

<sup>q</sup>psteglich@th-wildau.de

\* Corresponding author

**Keywords:** CMOS, Mach-Zehnder, VLSI

**Abstract.** We designed and produced an integrated silicon photonic circuit, in a single chip with IHP SG25H4\_EPIC 0.25  $\mu\text{m}$  technology. A Mach-Zehnder interferometer with an alternative shape for better integration, together with a standard-shape Mach-Zehnder interferometer have been realized. In this work, preliminary results of comparative performance measurements between the two Mach-Zehnder interferometer are shown.

## Introduction

Silicon photonics is a rapidly emerging field in research and technology of photonic integrated circuits [1]. Given its high refraction index and low dispersion, silicon is a high quality material for light guiding devices. On the other hand, VLSI CMOS compatible processes allow one to design reliable photonic structures, which can be easily integrated with standard electronic circuits at affordable cost [2,3]. Several structures can be envisaged by means of Silicon Photonic technology [4] such as, for example, optical ring resonators [5,6] or Mach-Zehnder interferometers.

In the basic standard geometry of the Mach-Zehnder interferometer, the arm dimensions are too large for an efficient integration on a silicon chip, in applications where a large number of

interferometers are required such as in silicon pixel detectors used in many fields of science and applications - from particle and nuclear physics experiments to medical physics.

Optical modulation, in silicon photonic integrated Mach-Zehnder interferometers can be obtained using the interference condition between the two different interferometer branches by controlling the electro-optical effect (plasma dispersion) [7,8].

The silicon photonic integrated Mach-Zehnder, if available with a geometry that maximizes the integration on a silicon chip, is an excellent device for many applications that require integration of a large number of channels in a single chip. That allows realizing a chip that is able, together with the photonic element, to host electronics and sensors on silicon, such as high-speed data transmission in the high-energy particles silicon detectors. [9]

Two Mach-Zehnder interferometers with different configurations have been designed and produced in a single die in IHP SG25H4\_EPIC 0.25  $\mu\text{m}$  technology: one developed almost entirely in line (A configuration), while the second has the two arms folded in a spiral to minimize the occupied surface (B configuration) as shown in Figure 1.

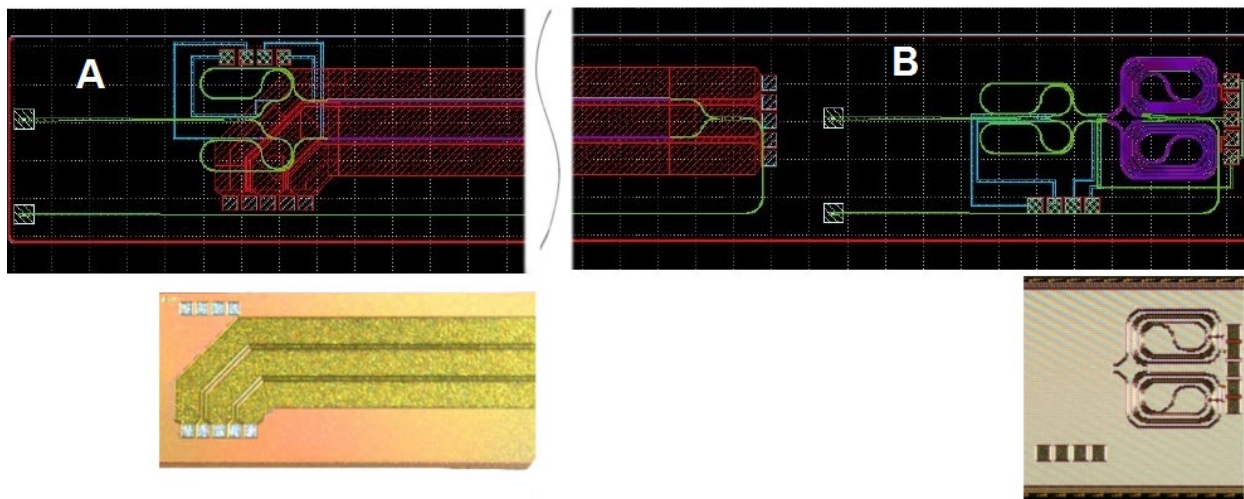


*Figure 1: Two Mach-Zehnder interferometers with different geometric configuration in a single die. On the left is the standard straight configuration (A) while on the right there is a spiral configuration (B). On the top, the layout drawings are visible; on the bottom are pictures of details corresponding to devices.*

The spiral configuration (1300  $\mu\text{m}$  x 700  $\mu\text{m}$ ), with respect to the standard straight one (6200  $\mu\text{m}$  x 600  $\mu\text{m}$ ), offers smaller size which allows easier integration.

### **Test setup**

The two different Mach-Zehnder interferometers have been tested in the laboratory and their performances have been compared in a 1550 nm optical telecommunication window.

The optical and electrical contact positioning has been carried out by means of micrometric movements on three perpendicular axes.

### **Measurements and test results.**

The first test consists in a transmission spectrum measurement around the typical wavelength window in the absence of electrical polarization ( $V = 0$  Volt), as shown in Figure 2 and Figure 3.

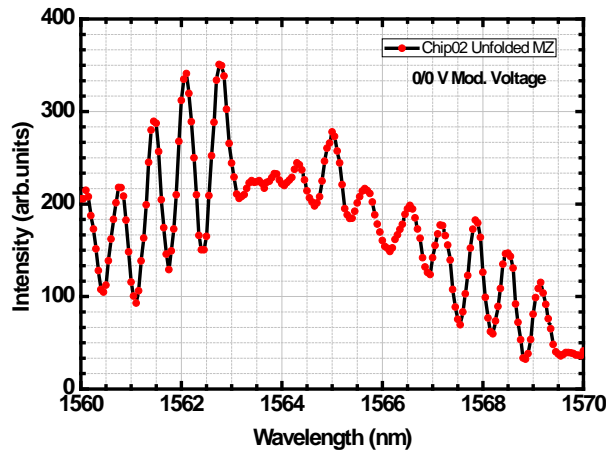


Figure 2: Unfolded Mach-Zehnder interferometer transmission spectrum.

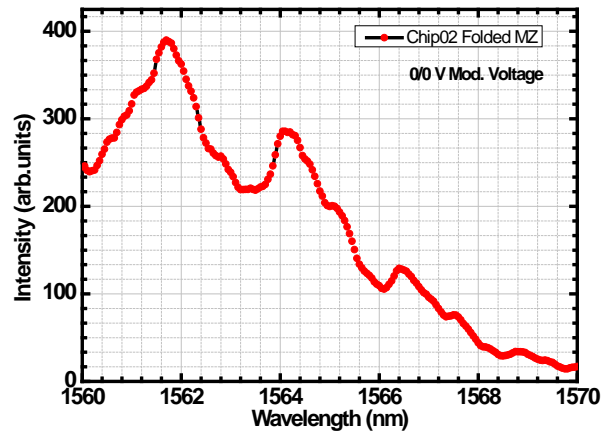


Figure 3: Folded Mach-Zehnder interferometer transmission spectrum.

The oscillation of the transmitted intensity at different wavelengths is due to frequency dependent dephasing of the light transmitted along the two arms of the Mach-Zehnder. The second test consists in a modulation scan carried out at wavelength fixed by applying a reverse potential ramp (0V / 3V) to a single interferometer Mach-Zehnder arm as shown in Figure 4 and Figure 5.

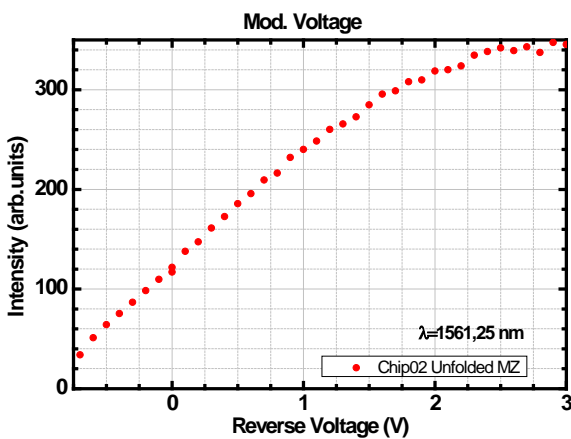


Figure 4: Unfolded Mach-Zehnder interferometer modulation scan vs. potential ramp.

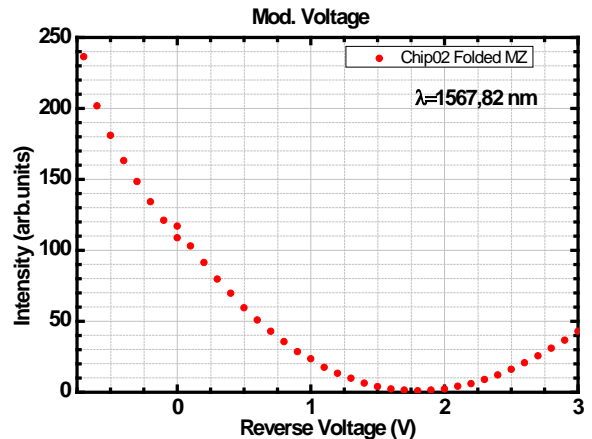


Figure 5: Folded Mach-Zehnder interferometer modulation scan vs. potential ramp.

In both cases, a large area of linear modulation of the signal is clearly shown as a function of the applied potential. The signal is coupled and transmitted with good efficiency in the optical circuit.

The last test performed was to observe the dynamic modulation response of the Mach-Zehnder interferometer. A laser source injected the beam in the Mach-Zehnder and the output of the modulator optically was coupled with an ultrafast, InGaAs PIN photodetector Picometrix P-50A. The signal was amplified by a SHF 806 E modulator drive. The modulation was obtained

with a square wave applied to the modulator diodes. The results are shown in Figure 6, where the resulting modulation is clearly visible.

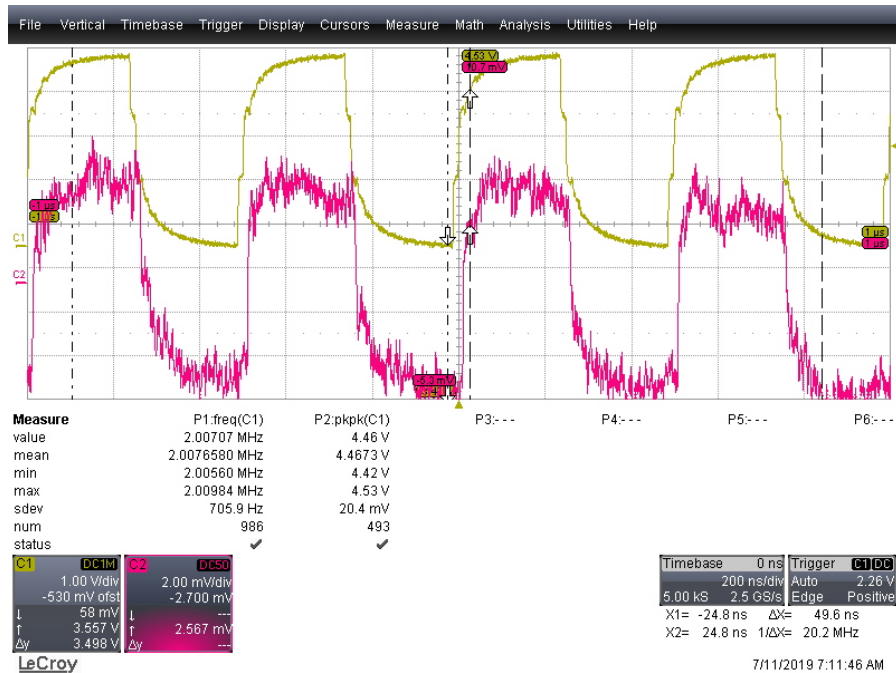


Figure 6: Acquisition from oscilloscope of the modulating electrical signal applied to the MZ junction and the resulting optical signal output from the MZ coupled with an InGaAs PIN photodetector Picometrix P-50A and amplified.

## Conclusions and Outlook

An integrated silicon photonic chip implementing two different Mach-Zehnder interferometers, in straight and folded configurations, was produced in a single die in IHP SG25H4\_EPIC 0.25  $\mu\text{m}$  technology. Some preliminary tests were performed and both Mach-Zehnder interferometers showed clear electro-optical modulation. More detailed high speed bit error rate data transmission tests with standard telecom pseudo random binary sequences are foreseen to validate the design. The folded Mach-Zehnder interferometer, given its reduced footprint, represents a promising device in many space critical applications.

## Acknowledgements

The authors want to thank Dr. Lisa Noetzel who reviewed the paper.

## References

- [1] P. Steglich and F. De Matteis, "Introductory Chapter: Fiber Optics" In Fiber optics Ed. P. Steglich, IntechOpen, (2019) ISBN: 978-1-83881-156-3. <https://doi.org/10.5772/intechopen.74877>
- [2] R. Russo et al., Toward optical and superconducting circuit integration, Supercond. Sci. Tech., 17(5), S456-S459 (2004) 45. <https://doi.org/10.1088/0953-2048/17/5/074>

- [3] P. Steglich et al., Hybrid-Waveguide Ring Resonator for Biochemical Sensing, *IEEE Sensors J.*, 17(15), 4781-4790 (2017). <https://doi.org/10.1109/JSEN.2017.2710318>
- [4] F. Bonaccorso et al, Graphene photonics and optoelectronics, *Nat Photonics* 4, 611–622 (2010). <https://doi.org/10.1038/nphoton.2010.186>
- [5] G. Alimonti, et al., Use of silicon photonics wavelength multiplexing techniques for fast parallel readout in high energy physics, *Nuclear Inst. and Methods in Physics Research: A*, 936, 601 (2019). <https://doi.org/10.1016/j.nima.2018.09.088>
- [6] P. Proposito et al, UV-nanoimprinting lithography of Bragg Gratings on hybrid sol-gel based channel waveguides, *Solid State Sci.* 12, 1886-1889 (2010). <https://doi.org/10.1016/j.solidstatesciences.2010.03.014>
- [7] R. A. Soref and B.R. Bennett, Electrooptical effects in silicon, *IEEE J Quantum Elect* QE-23 (1), 123, (1987). <https://doi.org/10.1109/JQE.1987.1073206>
- [8] G.T. Reed and E.J.Png, Silicon optical modulators, *Mater.Today*, 8(1), 40-50 (2005). [https://doi.org/10.1016/S1369-7021\(04\)00678-9](https://doi.org/10.1016/S1369-7021(04)00678-9)
- [9] E. Cortina Gil et al., The beam and detector of the NA62 experiment at CERN, *JINST* 12 P05025 (2017).